SCIENTIFIC REPORTS

Correction: Retraction

OPEN

Identification of a novel Na^+-coupled Fe^{3+}-citrate transport system, distinct from mammalian INDY, for uptake of citrate in mammalian cells

Received: 3 November 2017
Accepted: 22 January 2018
Published online: 06 February 2018

Jiro Ogura[1], Ellappan Babu[1], Seiji Miyauchi[2], Sabarish Ramachandran[1], Elizebeta Nemeth[3], Yangzom D. Bhutia[1] & Vadivel Ganapathy[1]

NaCT is a Na^+-coupled transporter for citrate expressed in hepatocytes and neurons. It is the mammalian ortholog of INDY (I'm Not Dead Yet), a transporter which modifies lifespan in *Drosophila*. Here we describe a hitherto unknown transport system for citrate in mammalian cells. When liver and mammary epithelial cells were pretreated with the iron supplement ferric ammonium citrate (FAC), uptake of citrate increased >10-fold. Iron chelators abrogated the stimulation of citrate uptake in FAC-treated cells. The iron exporter ferroportin had no role in this process. The stimulation of citrate uptake also occurred when Fe^{3+} was added during uptake without pretreatment. Similarly, uptake of Fe^{3+} was enhanced by citrate. The Fe^{3+}-citrate uptake was coupled to Na^+. This transport system was detectable in primary hepatocytes and neuronal cell lines. The functional features of this citrate transport system distinguish it from NaCT. Loss-of-function mutations in NaCT cause early-onset epilepsy and encephalopathy; the newly discovered Na^+-coupled Fe^{3+}-citrate transport system might offer a novel treatment strategy for these patients to deliver citrate into affected neurons independent of NaCT. It also has implications to iron-overload conditions where circulating free iron increases, which would stimulate cellular uptake of citrate and consequently affect multiple metabolic pathways.

Mammalian cells express three SLC (solute-linked carrier)-type transporters that are responsible for the transfer of citric-acid cycle intermediates across the plasma membrane; these are SLC13A2 (NaDC1 or Na^+-coupled dicarboxylate transporter 1), SLC13A3 (NaDC3 or Na^+-coupled dicarboxylate transporter 2) and SLC13A5 (NaCT or Na^+-coupled citrate transporter)[1,2]. SLC13A2 and SLC13A3 show much higher affinity towards dicarboxylates (e.g., succinate) than towards tricarboxylates (e.g., citrate). In contrast, SLC13A5 exhibits greater affinity towards citrate than towards dicarboxylates. SLC13A5 is the mammalian ortholog of *Drosophila* Indy[3,4], which is a critical determinant of life span[5]. Deletion of Slc13a5 in mouse protects against diet-induced obesity, insulin resistance, and metabolic syndrome[6]. This is most likely related to the function of the transporter in hepatic lipid synthesis as the transporter is expressed robustly in liver[4,7,8]; the expression is restricted to the blood-facing sinusoidal membrane in hepatocytes[9] and the transporter promotes incorporation of extracellular citrate into lipids in these cells[10]. As such, deletion of the transporter probably mimics caloric restriction in the liver, thus providing protection against obesity, insulin resistance, and metabolic syndrome. While loss of the transporter function in liver has a beneficial effect on the organism, it might not be the case in other tissues where the transporter is expressed. Loss-of-function mutations in human SLC13A5 are associated with severe childhood epilepsy[11–16]; [reviewed in refs[17,18]]. This transporter was first cloned from rat brain in mammals[4]; its expression is restricted to neurons in specific regions of the brain[4,19]. The robust expression of the transporter in the brain explains the drastic consequences of the loss-of-function mutations in this transporter.

[1]Department of Cell Biology and Biochemistry, Texas Tech University Health Sciences Center, Lubbock, TX, 79430, USA. [2]Department of Pharmaceutics, Toho University, Funabashi, Chiba, 274-8510, Japan. [3]Department of Medicine and Center for Iron Disorders, University of California at Los Angeles, Los Angeles, CA, 90095, USA. Correspondence and requests for materials should be addressed to V.G. (email: Vadivel.ganapathy@ttuhsc.edu)

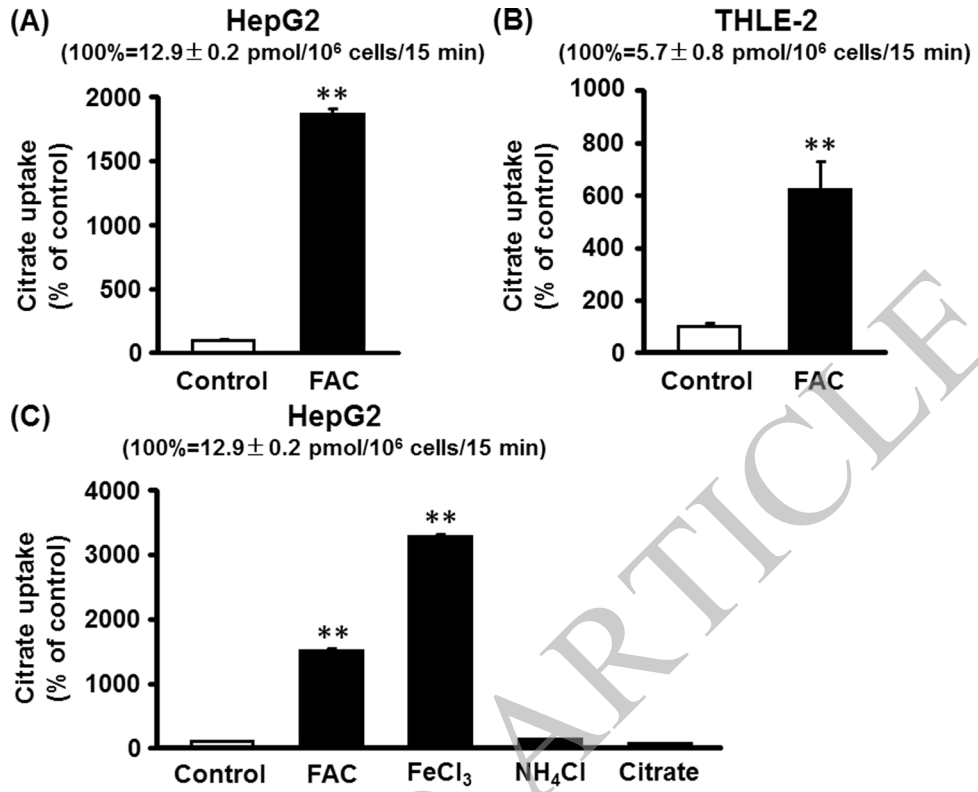

Figure 1. Effect of pretreatment with Fe^{3+} on citrate uptake in a human hepatocarcinoma cell line and a human normal hepatocyte cell line. The human hepatocarcinoma cell line HepG2 (**A**) and the human normal hepatocyte cell line THLE-2 (**B**) were cultured in the absence or presence of FAC (65 μg/ml) for two passages. The cells were then seeded for uptake measurements and cultured in the absence or presence of FAC; confluent cells were used for [^{14}C]-citrate (3.5 μM) uptake (NaCl buffer, pH 7.5; 15 min incubation). (**C**) HepG2 cells were cultured in the absence or presence of FAC (250 μg/ml), $FeCl_3$ (1 mM), NH_4Cl (1 mM) or citrate (1 mM) for two passages. The cells were then seeded for uptake measurements and cultured in the absence or presence of FAC, $FeCl_3$, NH_4Cl or citrate. Confluent cells were used for [^{14}C]-citrate (3.5 μM) uptake (NaCl buffer, pH 7.5; 15 min incubation). $^{**}p < 0.01$.

To the best of our knowledge, SLC13A5 is the only plasma membrane transporter known thus far that is selective for Na^+-coupled citrate uptake in mammalian cells. Here we report on the identification of a novel, hitherto unknown, transport system for citrate uptake in mammalian cells. This newly discovered transport system mediates Fe^{3+}-coupled citrate uptake in a Na^+-dependent manner. This transporter is unequivocally different from SLC13A5.

Results

Citrate uptake in control and FAC (ferric ammonium citrate)-treated liver cells. Our original aim was to determine if chronic exposure of liver cells to excess iron influences the expression and function of NaCT. For this, we exposed HepG2 cells, which express NaCT[9,10], and also the non-tumorigenic human hepatocyte cell line THLE-2 to ferric ammonium citrate (FAC) as an iron supplement; we cultured the cells in the presence of 65 μg/ml FAC for two passages and then used the cells for citrate uptake in the presence of NaCl to monitor NaCT function. There was a marked increase in citrate uptake in HepG2 cells (Fig. 1A) and THLE-2 cells (Fig. 1B) as a result of chronic exposure to FAC. The increase in uptake was 18-fold in HepG2 cells and 6-fold in THLE-2 cells. As FAC contains ferric ion, ammonium ion and citrate, we cultured HepG2 cells with FAC (250 μg/ml), $FeCl_3$ (1 mM), NH_4Cl (1 mM), or citrate (1 mM) for two passages, and then used the cells for citrate uptake. Only treatment with FAC and $FeCl_3$ increased citrate uptake compared to untreated cells (Fig. 1C).

Non-involvement of NaCT in citrate uptake induced by FAC treatment. Human NaCT is stimulated by Li^+ [10,20]. To determine if the citrate uptake that was enhanced by FAC treatment occurred via NaCT, we measured citrate uptake in control and FAC-treated HepG2 cells in the absence and presence of 10 mM LiCl. In control cells, Li^+ stimulated citrate uptake 5-fold as expected of the NaCT (Fig. 2A). FAC treatment increased citrate uptake several fold, but the effect of Li^+ was minimal in FAC-treated cells (Fig. 2A). If the citrate uptake in control cells was subtracted from that in FAC-treated cells, the activity that was enhanced by FAC treatment was less in the presence of Li^+. We then used the human breast cancer cell line MCF7; these cells do not express NaCT irrespective of whether or not the cells were exposed to FAC (250 μg/ml) (Fig. 2B). We then used control and FAC-exposed cells for citrate uptake. In control cells, citrate uptake was very low compared to HepG2 cells

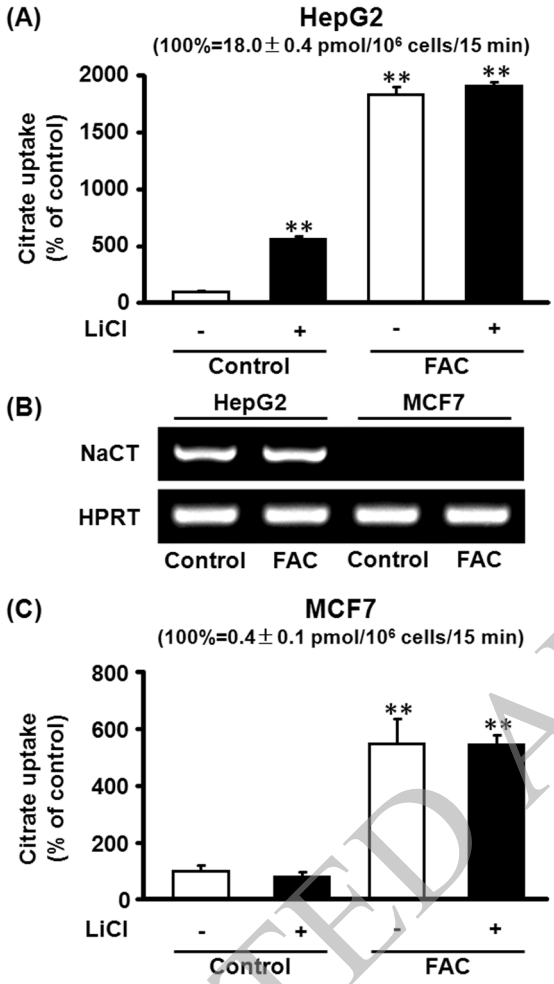

Figure 2. Non-involvement of NaCT in citrate uptake stimulated by FAC pretreatment. (**A**) HepG2 cells were cultured in the absence or presence of FAC (250 μg/ml) for two passages. The cells were then seeded for uptake measurements and cultured in the absence or presence of FAC; confluent cells were used for [^{14}C]-citrate (3.5 μM) uptake (NaCl buffer, pH 7.5; 15 min incubation) in the absence or presence of 10 mM LiCl. (**B**) RT-PCR for expression of NaCT mRNA in control and FAC-treated HepG2 and MCF7 cells. The PCR products from both cell lines were run on the same gel to detect NaCT or HPRT (The images of the entire gels are given in Supplementary Fig. S7). (**C**) MCF7 cells were cultured in the absence or presence of FAC (250 μg/ml) for two passages. The cells were then seeded for uptake measurements and cultured in the absence or presence of FAC; confluent cells were used for [^{14}C]-citrate (3.5 μM) uptake (NaCl buffer, pH 7.5; 15 min incubation) in the absence or presence of 10 mM LiCl. $^{**}p < 0.01$.

(0.4 ± 0.1 pmol/10^6 cells/15 min in MCF7; 18.0 ± 0.4 pmol/10^6 cells/15 min in HepG2) and was insensitive to Li^+ (Fig. 2C). In FAC-treated cells, citrate uptake increased 6-fold and Li^+ had little effect (Fig. 2C). As there was no evidence of NaCT mRNA in MCF7 cells with or without exposure to FAC, the presence of robust citrate uptake in FAC-treated cells indicates that the observed uptake activity is unrelated to NaCT.

Direct stimulation of citrate uptake by Fe^{3+}. In studies described above, the cells were treated with FAC and then citrate uptake was measured in the absence of Fe^{3+}. To determine if Fe^{3+} could stimulate citrate uptake directly when added to the uptake buffer, citrate uptake was measured in HepG2 cells without prior treatment with FAC; FAC (250 μg/ml), $FeCl_3$ (1 mM), NH_4Cl (1 mM), or citrate (1 mM) were added directly to the uptake buffer. $FeCl_3$, but not any of the other three compounds, increased citrate uptake (Supplementary Fig. S1), showing the direct stimulatory effect of Fe^{3+} on citrate uptake. It was also important to note that pretreatment with FAC stimulated [^{14}C]-citrate uptake (Fig. 1C) whereas it did not have any effect when added directly to the uptake medium (Supplementary Fig. S1). The most likely explanation for this difference is the fact that FAC is a complex of Fe^{3+}, NH_4^+, and citrate, and therefore the unlabeled citrate suppresses [^{14}C]-citrate by competition in spite of the presence of Fe^{3+}. This is not the case when cells are exposed to FAC only during pretreatment but not during uptake.

Dose-response relationship for the stimulation of citrate uptake by Fe^{3+}. The plasma concentration of free Fe^{3+} is in low micromolar range even under conditions of iron overload[21,22]. Therefore, to determine if the stimulation of citrate uptake could occur at concentrations of Fe^{3+} that are relevant to physiological and

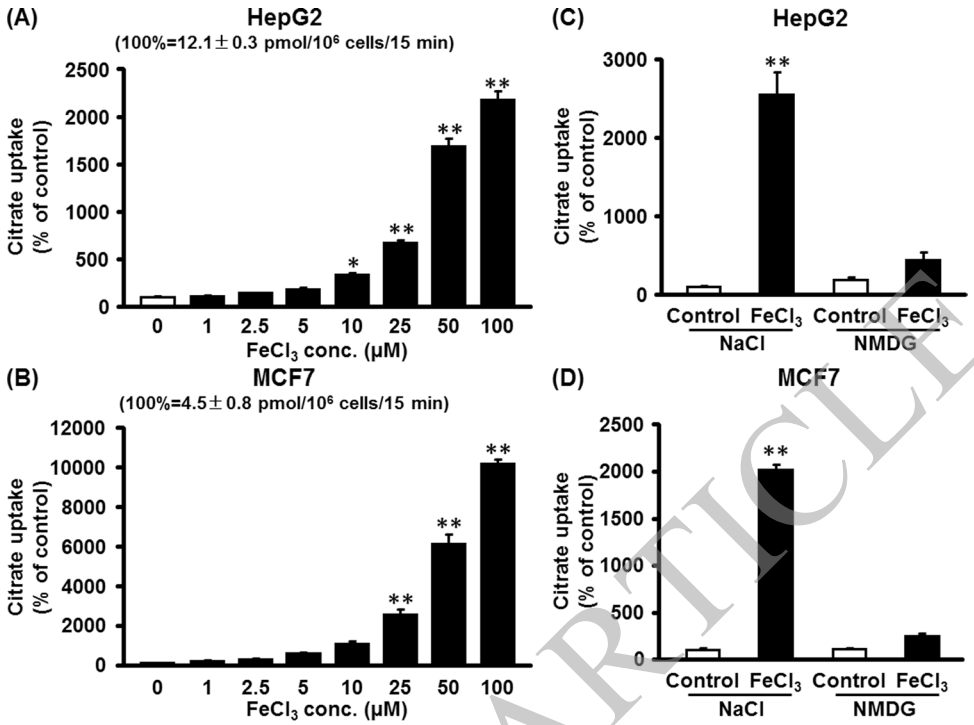

Figure 3. Fe^{3+} dose-response for stimulation for citrate uptake and the Na^+-dependence of the uptake process in HepG2 cells and MCF7 cells. HepG2 (**A**) and MCF7 cells (**B**) were cultured to confluence and then used for measurements of [^{14}C]-citrate (3.5 μM) uptake (NaCl buffer, pH 7.5; 15 min incubation) in the presence of increasing concentrations of Fe^{3+} ($FeCl_3$). HepG2 (**C**) and MCF7 cells (**D**) were cultured to confluence and then used for measurement of Fe^{3+} (50 μM)-stimulated citrate uptake in the presence (NaCl buffer, pH 7.5) or absence of Na^+ (NMDG chloride, pH 7.5) using [^{14}C]-citrate (3.5 μM). Data are presented as percent of control uptake measured in the presence of Na^+ but in the absence of Fe^{3+}. *$p < 0.05$; **$p < 0.01$.

pathological conditions, we performed a dose-response study in HepG 2 cells (Fig. 3A) and MCF7 cells (Fig. 3B). We found significant stimulation of citrate uptake even at [Fe^{3+}] as low as 2.5 μM when directly compared with uptake in the absence of Fe^{3+} (paired Student's t test; $p < 0.05$). The stimulation increased as [Fe^{3+}]increased even up to 100 μM. As iron can exist in two different ionic forms (Fe^{2+} and Fe^{3+}), we tested the relative efficacy of the two forms in stimulating citrate uptake in MCF7 cells. When present at equal concentration (50 μM), the potency of Fe^{3+} to stimulate citrate uptake was at least 2-fold greater than the potency of Fe^{2+} (Supplementary Fig. S2A).

Obligatory Na^+ requirement for the Fe^{3+}-stimulated citrate transport system. NaCT is obligatorily dependent on Na^+. To determine if the newly discovered Fe^{3+}-stimulated citrate transport system is also dependent on Na^+, we monitored Fe^{3+}-stimulated citrate uptake in the presence and absence of Na^+ in HepG2 cells and MCF7 cells. Here we substituted NaCl in the uptake buffer iso-osmotically with *N*-methyl-D-glucamine chloride, thus replacing Na^+ with a bulky organic cation. The robust Fe^{3+}-stimulated citrate uptake activity was present in both cell lines when measured in the presence of NaCl, but the activity was nearly undetectable in the absence of Na^+ (Fig. 3C,D). To determine if Na^+ could be replaced with other monovalent inorganic ions, we studied the ability of Li^+ and K^+ to substitute for Na^+ to support Fe^{3+}-stimulated citrate uptake. We found Li^+ to be equally potent as Na^+ in supporting Fe^{3+}-stimulated citrate uptake in MCF7 cells (Supplementary Fig. S2B). K^+ was also able to substitute for Na^+ almost to the same extent.

Substrate selectivity of Fe^{3+}-stimulated citrate transport system. Human NaCT is almost exclusive for citrate[7]. We determined the substrate selectivity of the Fe^{3+}-stimulated citrate transport system by monitoring the ability of various carboxylates (2.5 mM) to compete with [^{14}C]-citrate (3.5 μM) for uptake in the presence of $FeCl_3$ (50 μM) in human cell lines. In HepG2 cells (Fig. 4A) and MCF7 cells (Fig. 4B), only citrate and malate competed with [^{14}C]-citrate for uptake via the Fe^{3+}-stimulated transport system. Lactate, pyruvate, and succinate had no (MCF7) or minimal (HepG2) effect.

Differential interaction of NaCT and Fe^{3+}-stimulated citrate transport system with isocitrate. NaCT recognizes citrate but not isocitrate as a substrate[7]. To determine if the Fe^{3+}-stimulated citrate transport system interacts with isocitrate, we evaluated the ability of isocitrate to compete with [^{14}C]-citrate for uptake in HepG2 cells in the absence or presence of 50 μM $FeCl_3$. In these cells, the uptake of [^{14}C]-citrate in the absence of Fe^{3+} occurs solely via NaCT whereas it occurs predominantly via the Fe^{3+}-stimulated transport system in the presence of $FeCl_3$. Unlabeled citrate competed with [^{14}C]-citrate for NaCT-mediated uptake at millimolar

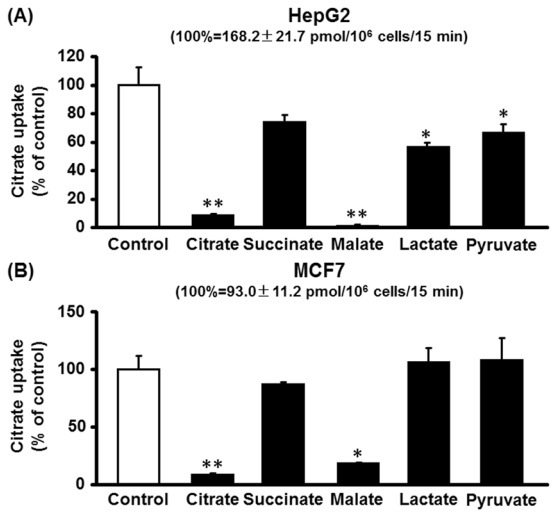

Figure 4. Substrate selectivity of the citrate transport system that is stimulated in HepG2 cells and MCF7 cells by Fe^{3+}. HepG2 (**A**) and MCF7 cells (**B**) were cultured to confluence prior to uptake measurements. Uptake of [^{14}C]-citrate (3.5 μM) was measured in NaCl buffer, pH 7.5, for 15 min in the presence of $FeCl_3$ (50 μM) in absence or presence of the various carboxylates (2.5 mM). *$p < 0.05$; **$p < 0.01$.

concentrations (Supplementary Fig. S3A). This was as expected because NaCT in HepG2 cells is a low-affinity transporter with the Michaelis constant in millimolar range[9]. Isocitrate did not have any effect on [^{14}C]-citrate uptake at 1 mM (Supplementary Fig. S3B). In contrast, when [^{14}C]-citrate uptake was measured in the presence of Fe^{3+}, the uptake was inhibited markedly by unlabeled citrate as well as by isocitrate even at micromolar concentrations (Supplementary Fig. S3C,D).

Human NaCT is stimulated by Li^+, and the stimulation is associated with an increase in the affinity of the transporter for citrate[10,20]. To demonstrate unequivocally that human NaCT interacts with citrate but not isocitrate, we measured the transport activity of NaCT in HepG2 cells in the presence of 10 mM Li^+ and examined the effects of unlabeled citrate and isocitrate on [^{14}C]-citrate uptake. The results were as predicted; unlabeled citrate inhibited [^{14}C]-citrate uptake markedly (80–90%) even at 1 mM. This was in contrast to the findings described above in the absence of Li^+ because of the ability of Li^+ to increase the affinity of NaCT to citrate. But even in the presence of Li^+, the NaCT-mediated uptake of citrate was not inhibited by isocitrate. These findings demonstrate that NaCT does not interact with isocitrate, but the Fe^{3+}-stimulated citrate transport system interacts with isocitrate as well as citrate with high affinity. The same substrate specificity was observed for the citrate uptake system that was stimulated in HepG2 cells and MCF7 cells by chronic treatment with FAC.

Effect of Li^+ on Na^+-coupled Fe^{3+}-citrate transport system. The data in Fig. 2 describe the effect of Li^+ on the activity of Na^+-coupled Fe^{3+}-citrate transport system in HepG2 cells and MCF7 cells, but in that experiment the activity of the transport system was monitored in FAC-exposed cells without adding Fe^{3+} directly to the uptake medium. The effect of Li^+ on the transport activity was not consistent; the activity appeared to be inhibited by Li^+ in HepG2 cells but there was no noticeable effect in MCF7 cells. As the exact mechanism by which the Na^+-coupled Fe^{3+}-citrate uptake gets activated in FAC-treated cells is not known, we examined the Li^+ effect on the transport system in MCF7 cells by measuring the transport activity in cells without prior exposure to FAC but in the presence of Fe^{3+} directly added to the uptake medium. We chose MCF7 cells to avoid any confounding influence of NaCT on data interpretation as these cells showed no evidence of NaCT mRNA. As expected, there was not measurable citrate uptake in the presence or absence of Li^+ when Fe^{3+} was not present in the uptake medium (Supplemental Fig. S4). There was however robust citrate uptake in the presence of Fe^{3+}, and the activity increased further by ~40% in the presence of 10 mM Li^{3+} (Supplementary Fig. S4). The magnitude of increase in activity with 10 mM Li^+ was very small compared the increase in NaCT activity at the same concentration of Li^+ (~500%, Fig. 2A). The data in Fig. S4 were difficult to interpret to some degree because Li^+ is capable of substituting for Na^+ with equal potency for this transport system (Supplementary Fig. S2). If 140 mM Na^+ used in these experiments was not a saturating concentration for maximal citrate uptake, addition of 10 mM Li^+ would increase the uptake activity by simply increasing the concentration of the co-transported ion (Na^+ plus Li^+). To determine if this was the case, we investigated the Na^+-saturation kinetics for the transport system in MCF7 cells. The uptake of citrate was measured in the presence of Fe^{3+} (50 μM) and in the presence of increasing concentration of Na^+. Here *N*-methyl-D-glucamine substituted for Na^+ iso-osmotically. The uptake activity increased with increasing concentration of Na^+, and the activity did not saturate even at 140 mM Na^+ (Supplementary Fig. S5). Based on these data, we conclude that the Na^+-coupled Fe^{3+}-citrate transport system operates equally well with Li^+ in place of Na^+ and that Li^+ does not activate the transport system as it does in the case of NaCT.

Mechanism of stimulation of citrate uptake in FAC-treated cells. As the new citrate transport system is detectable in FAC-treated cells in the absence of exogenous addition of Fe^{3+} in the uptake medium, it raises the question as to the mechanism of this uptake activity. We speculated that the treatment of the cells with FAC

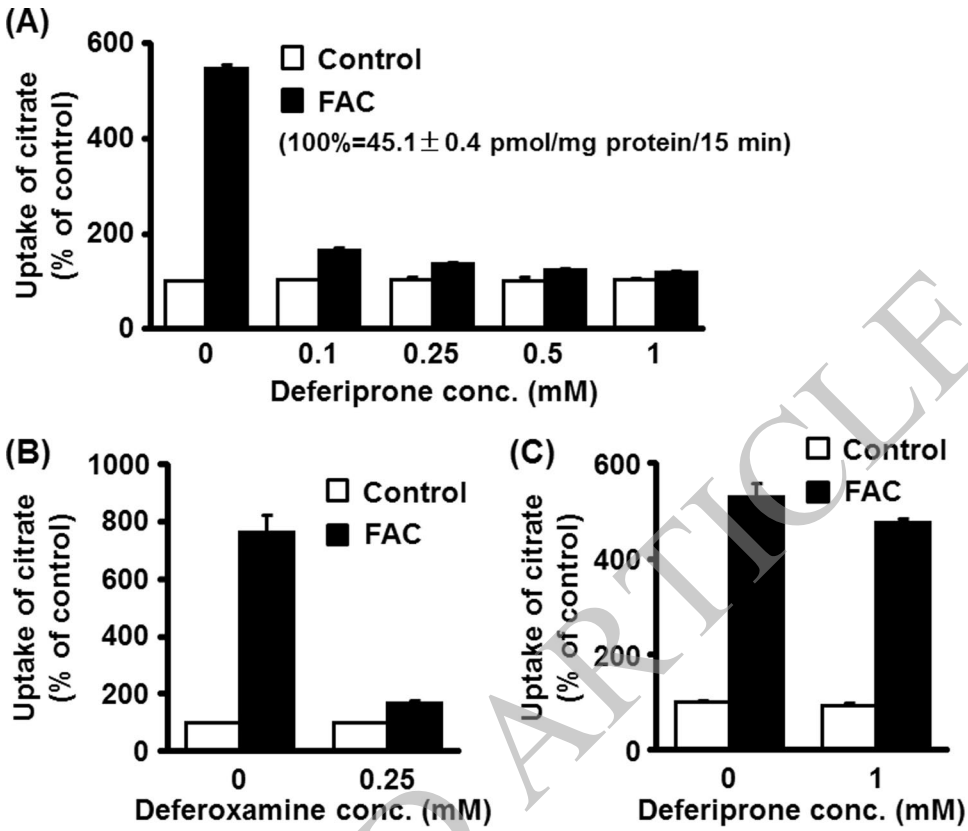

Figure 5. Effects of iron chelators on Fe^{3+}-stimulated citrate uptake in FAC-treated HepG2 cells. HepG2 cells were cultured in the absence or presence of FAC (250 μg/ml) for two passages. The cells were then seeded in 24-well plates and cultured in the absence or presence of FAC (250 μg/ml) to confluence prior to uptake measurement. Uptake of [^{14}C]-citrate (3.5 μM) was measured in a NaCl buffer, pH 7.5 for 15 min in the absence or presence of increasing concentrations of deferiprone, a cell-permeable iron chelator (**A**) or 0.25 mM deferoxamine, a cell-impermeable iron chelator (**B**). (**C**) HepG2 cells were cultured in the absence or presence of FAC (250 μg/ml) for two passages. The cells were then seeded in 24-well plates and cultured in the absence or presence of FAC (250 μg/ml) to confluence and then exposed to 1 mM deferoxamine prior to uptake measurement for 30 min. Uptake of [^{14}C]-citrate (3.5 μM) was then measured in these cells in a NaCl buffer, pH 7.5 for 15 min in the absence of the iron chelator.

leads to accumulation of Fe^{3+} inside the cells and that when the cells are washed to remove extracellular FAC and then used to measure citrate uptake, Fe^{3+} effluxes from the cells and stimulates citrate uptake. We tested the validity of this hypothesis using deferiprone, a cell-permeable iron chelator. Control and FAC-treated HepG2 cells were used for citrate uptake in the absence and presence of deferiprone. In control cells without pretreatment with FAC, deferiprone did not have any effect on citrate uptake because the activity of the newly discovered citrate transport system was negligible when monitored in the absence of Fe^{3+} (Fig. 5A). In FAC-treated cells, the citrate transport activity was robust without the addition of Fe^{3+} during uptake. However, this transport activity was almost completely blocked by deferiprone in the uptake buffer (Fig. 5A). Similar results were obtained with deferoxamine, a cell-impermeable iron chelator (Fig. 5B).

There could be two different explanations for these findings. First, Fe^{3+} effluxes out of the cells to stimulate citrate uptake; second, FAC is adhered to the extracellular surface of the cells during FAC treatment, which then serves as the source of Fe^{3+} to stimulate citrate uptake. To differentiate between these two possibilities, we treated control and FAC-exposed cells with deferiprone for 15 min prior to initiation of citrate uptake to remove any Fe^{3+} that was adhered to the cell surface and then measured citrate uptake without adding any exogenous source of Fe^{3+}, but in the absence of the iron chelator. This maneuver had no effect on citrate uptake; the increase in citrate uptake in FAC-treated cells was still detectable (Fig. 5C), suggesting that Fe^{3+} effluxes out of the FAC-treated HepG2 cells during uptake measurement, which then stimulates citrate uptake.

Non-involvement of ferroportin in the efflux of Fe^{3+} in FAC-treated HepG2 cells. To date, ferroportin is the only transporter in the plasma membrane of mammalian cells that effluxes iron, but in the form of Fe^{2+}, which then gets oxidized to Fe^{3+} by cell-surface ferroxidases[23]. To determine if this process is involved in the stimulation of citrate uptake in FAC-treated cells, we treated the FAC-exposed HepG2 cells with the synthetic minihepcidin peptide PR73 (1 μM) for 24 h. Hepcidin interacts with ferroportin and promotes its degradation; PR73 is a hepcidin mimetic that also binds to ferroportin and promotes its degradation[24]. In the absence of PR73, citrate uptake was several-fold higher in FAC-treated cells than in control cells (Fig., 6A). When the cells were

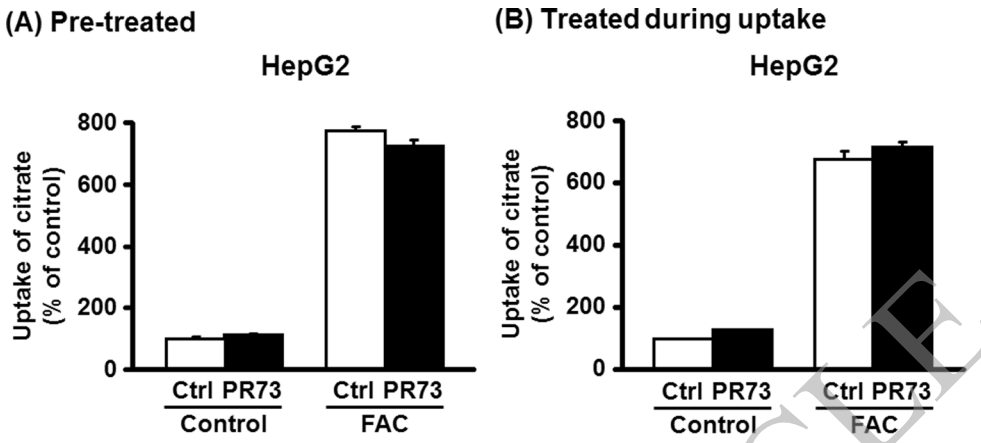

Figure 6. Influence of hepcidin mimetic minipeptide (PR73) on citrate uptake in FAC-treated HepG2 cells. HepG2 cells were cultured in the absence or presence of FAC (250 μg/ml) for two passages. (**A**) Prior to seeding of the cells for uptake measurements, the cells were treated with or without PR73 (1 μM) for 24 h. The cells were then prepared for uptake measurements. Uptake of [^{14}C]-citrate (3.5 μM) was measured in a NaCl buffer, pH 7.5 for 15 min. (**B**) Control and FAC-treated cells were also used citrate uptake without pretreatment in the presence of PR73, but uptake was measured with PR73 present in the uptake medium during the measurement of citrate uptake.

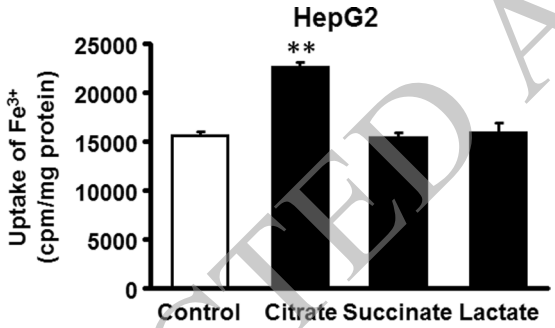

Figure 7. Stimulation of Fe^{3+} uptake by citrate in HepG2 cells. Uptake of [^{59}Fe]-$FeCl_3$ was measured in HepG2 cells in NaCl buffer, pH 7.5 (15 min incubation) in the absence or presence of 50 μM citrate, succinate or lactate. The results are expressed as counts/min/mg of protein. $^{**}p < 0.01$.

treated with PR73 prior to initiation of uptake, there was no change in citrate uptake. Immunofluorescence studies confirmed the reduced intensity of ferroportin in these cells (Supplementary Fig. S6). As hepcidin binds to ferroportin on the extracellular surface, hepcidin may simply mask the transport site of ferroportin, thus blocking the efflux of iron as a potential additional mechanism for the hepcidin-mediated blockade of ferroportin. Therefore, we monitored citrate uptake in control and FAC-treated HepG2 cells with PR73 present during uptake (no pretreatment). PR73 did not have any effect on citrate uptake in control cells and in FAC-treated cells under these conditions (Fig. 6B).

Stimulation of Fe^{3+} uptake by citrate. We then asked whether Fe^{3+} acted as an activator or a co-transported ion in the citrate uptake process. For this, we studied the effect of citrate on Fe^{3+} uptake in HepG2 cells. The uptake was measured using $^{59}Fe^{3+}$ in the form of $FeCl_3$ as the tracer. Fe^{3+} uptake was significantly stimulated by citrate (Fig. 7). Succinate and lactate, which do not interact with the transport system, failed to stimulate the uptake of Fe^{3+}.

Relevance of the zinc transporters to Fe^{3+}-stimulated citrate transport system. The functional features of the Fe^{3+}-stimulated citrate transport system indicate that the system mediates co-transport of Fe^{3+} and citrate in a Na^+-dependent manner. These features obviously qualify the transport system as an NTBI (non-transferrin-bound iron) transporter. NTBI exists predominantly in Fe^{3+} form. To date, the best-known NTBI transporter is the zinc transporter ZIP14, which transports NTBI in the form of Fe^{2+} following the conversion of Fe^{3+} into Fe^{2+} by cell-surface reductases[25–28]. ZIP8 is another zinc transporter capable of transporting Fe^{2+}[28]. We examined whether Zn^{2+} would substitute for Fe^{3+} to stimulate citrate uptake in MCF7 cells (Fig. 8A) as well as HepG2 cells (Fig. 8B). In both cell lines, $FeCl_3$ (75 μM) stimulated citrate uptake several fold as observed in previous experiments. In contrast, Zn^{2+} did not stimulate citrate uptake. Published reports indicate that Mn^{2+} is also a substrate for ZIP14 and ZIP8[28]; therefore, we tested the ability of this divalent metal ion to substitute for

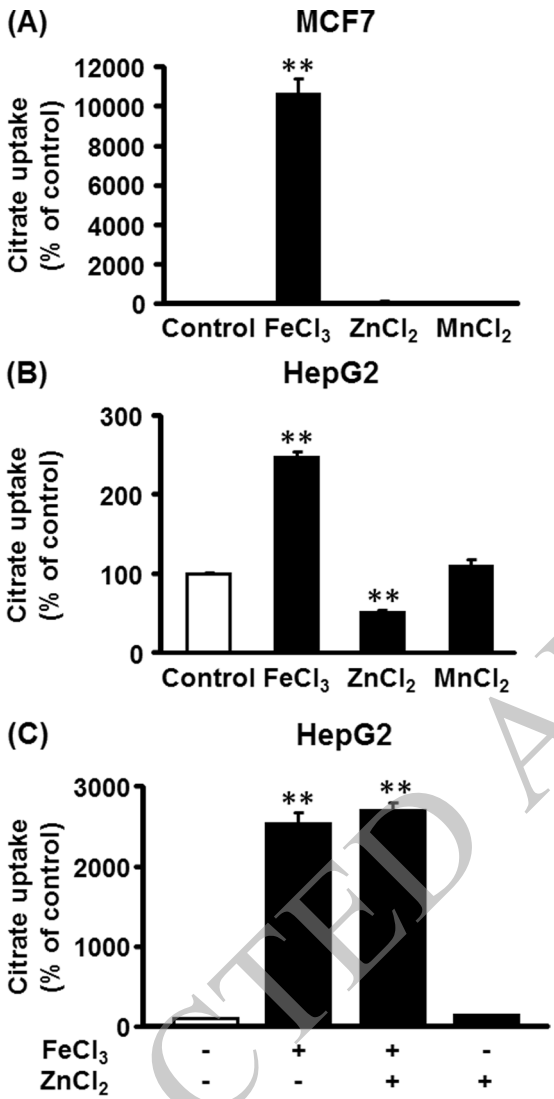

Figure 8. Effect of Zn^{2+} and Mn^{2+} on citrate uptake in MCF7 and HepG2 cells in the presence of Na^+. MCF7 cells (**A**) and HepG2 cells (**B**) were cultured to confluence and the cells were used to measure the uptake [^{14}C]-citrate (3.5 μM) for 15 min in the presence (NaCl buffer, pH 7.5) with $FeCl_3$ (50 μM), $ZnCl_2$ (50 μM), or $MnCl_2$ (50 μM). (**C**) HepG2 cells were cultured to confluence and the cells were then used to measure the uptake of [^{14}C]-citrate (3.5 μM) for 15 min in the presence (NaCl buffer, pH 7.5) and in the presence or absence of $FeCl_3$ (50 μM) or $ZnCl_2$ (50 μM) as indicated. The results are given as percent of control uptake measured in the absence of FeCl3. $^{**}p < 0.01$.

Fe^{3+} to support citrate uptake; again, this metal ion also was unable to stimulate citrate uptake (Fig. 8). We then examined if Zn^{2+} would impact on citrate uptake in the presence of Fe^{3+}; there was no effect of Zn^{2+} under these conditions either (Fig. 8C).

Expression of the Na^+-coupled Fe^{3+}-citrate transport system in primary hepatocytes and neuronal cell lines. We examined the expression of the newly discovered citrate transport system in primary hepatocytes prepared from mouse liver. Citrate uptake was measured in the presence and absence of Na^+ to detect NaCT function and in the presence of Na^+ and Fe^{3+} to detect the new citrate transport system (Fig. 9A). The uptake was 2-fold higher in the presence of Na^+ than in its absence (29.4 ± 0.4 versus 12.1 ± 0.2 pmol/mg of protein/15 min, respectively), providing evidence for NaCT. But the uptake in NaCl buffer increased ~45-fold when Fe^{3+} was present in the uptake buffer, providing evidence for the newly discovered citrate transport system. The Fe^{3+}-stimulated citrate uptake was significant even at Fe^{3+} concentrations as low as 2.5–5 μM (Fig. 9B). We then analyzed the kinetic parameters of Fe^{3+}-stimulated citrate transport system in these cells. To account for NaCT-mediated citrate uptake in these studies, we measured the uptake in NaCl buffer in the presence and absence of Fe^{3+}, and then subtracted the uptake measured in the absence of Fe^{3+} from the uptake measured in the presence of Fe^{3+}. This allowed determination of uptake activity that was specifically due to the newly identified Na^+-coupled Fe^{3+}-citrate transport system. The values for Michaelis constant and maximal velocity for the

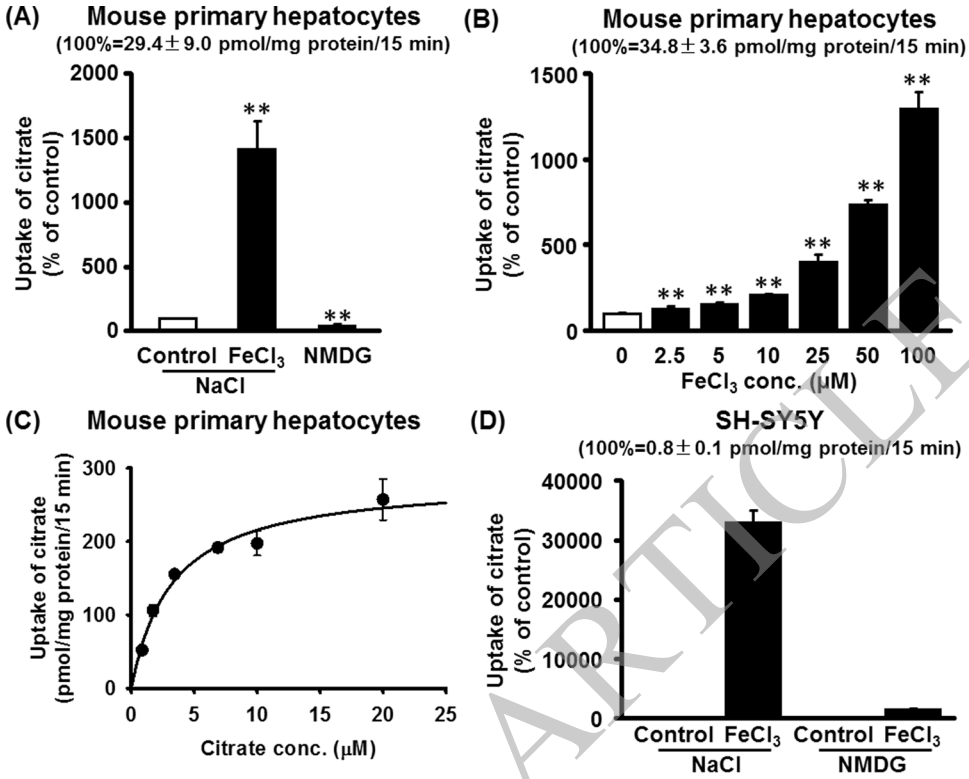

Figure 9. Expression of the Na^+-coupled Fe^{3+}-citrate uptake system in mouse primary hepatocytes and in a human neuronal cell line. (**A**) Hepatocytes were cultured to confluence and then used for measurement of [^{14}C]-citrate (3.5 μM) uptake in the presence (NaCl buffer, pH 7.5) with and without $FeCl_3$ (50 μM) or in the absence of Na^+ (NMDG chloride, pH 7.5). Data are presented as percent of control uptake measured in the presence of Na^+ but in the absence of Fe^{3+}. $^{**}p < 0.01$. (**B**) Dose-response for Fe^{3+} to stimulate [^{14}C]-citrate (3.5 μM) uptake in the presence (NaCl buffer, pH 7.5) in hepatocytes.$^{**}p < 0.01$. (**C**) Substrate saturation kinetics for the Na^+-coupled Fe^{3+}-citrate uptake in hepatocytes. (**D**) The human neuronal cell line SH-SY5Y was cultured to confluence and then used for measurement of [^{14}C]-citrate (3.5 μM) uptake in the presence (NaCl buffer, pH 7.5) with and without $FeCl_3$ (50 μM) or in the absence of Na^+ (NMDG chloride, pH 7.5). Data are presented as percent of control uptake measured in the presence of Na^+ but in the absence of Fe^{3+}.

transport system were 3.3 ± 0.6 μM and 285 ± 18 pmol/mg of protein/15 min (Fig. 9C). We also examined if this transport system is expressed in neuronal cell lines. We used the human neuroblastoma cell line SH-SY5Y for this purpose. These cells also showed robust functional activity for the newly discovered citrate transport system (Fig. 9D).

Discussion

To date, there has been no report in the literature on a transport system in the plasma membrane of mammalian cells other than NaCT that mediates the uptake of citrate. As such, the discovery of the new transport system for citrate is of biological significance. The functional features of this citrate transporter in the plasma membrane of mammalian cells are very different from those of NaCT. There are several lines of evidence indicating that this citrate transport system is distinct, both at the functional level and molecular level, from NaCT. First, citrate uptake via the new transport system is obligatorily dependent on Fe^{3+} whereas NaCT function is independent of Fe^{3+}. Second, even though the new transport system is Na^+-coupled, it is not selective for Na^+; Na^+ can be substituted with Li^+ or K^+ with almost equal potency; in contrast, NaCT is solely dependent on Na^+, and Li^+ cannot substitute for Na^+. Third, the impact of Li^+ on the two transport systems is very different. While Li^+ cannot substitute for Na^+ for NaCT, it activates the transport system in the presence of Na^+; this is not the case with the new citrate transport system. Fourth, the new transport system interacts with isocitrate whereas NaCT does not. Fifth, the affinity for citrate for the new transport system is at least two orders of magnitude greater than that for human NaCT (Michaelis constant for citrate: ~3 μM for the new transport system; ~650 μM for human NaCT). In addition to these significant functional differences that distinguish the new citrate transport system from NaCT, the data from MCF7 cells strongly suggest that the new transport system is likely to be also different from NaCT at the molecular level. In these cells, there is no detectable NaCT mRNA and there is no citrate uptake that is Na^+-coupled when measured in the absence of Fe^{3+}; even in the presence of Li^+, which has a marked stimulatory effect on human NaCT, Na^+-dependent citrate uptake is not detectable in these cells when monitored in the absence of Fe^{3+}. If NaCT were to be present in these cells, we should have been able to detect citrate uptake in the presence of Na^+ but in the absence of Fe^{3+}. Based on these data, we conclude that the Na^+-coupled Fe^{3+}-citrate uptake system described in this paper represents a new, hitherto unknown, citrate transporter in mammalian cells.

The newly discovered transport system mediates cellular uptake of not only citrate but also Fe^{3+}. This is an important feature as free iron in circulation exists almost entirely as Fe^{3+}-citrate chelate. While our present studies represent the first report on the presence of a Fe^{3+}-coupled citrate transport system in mammalian cells, the existence of such transport systems in microorganisms has been known for a long time [reviewed in ref.[29]]. These bacterial citrate transporters belong to the CitMHS family, which mediate metal-citrate complexes in symport with one or two H^+. Such transporters have been identified in *Streptococcus mutans*[30], *Streptomyces coelicolor*[31], and *Pseudomonas fluorescens*[32]. Interestingly, these bacterial metal-citrate transporters use not only Fe^{3+} but also divalent metal ions such as Mn^{2+}, Zn^{2+}, Ba^{2+}, Ca^{2+}, Pb^{2+}, and Ni^{2+}. It seems that one H^+ is involved in transport if the Fe^{3+}-citrate is the substrate and two H^+ are involved in transport if citrate complexed with a divalent metal ion is the substrate. The mammalian transporter is selective for Fe^{3+} in the formation of the metal-citrate complex; Fe^{2+} is able to substitute for Fe^{3+} but only with a significantly lesser potency. The other divalent metal ions such as Zn^{2+} and Mn^{2+} are unable to support the new transport system. This feature also suggests that the newly discovered iron transport system is distinct from ZIP8 and ZIP14, which can transport not only iron but also Zn^{2+} and/or Mn^{2+}. The preference of the new transport system for the trivalent iron is also unique because all other transporters that are known to transport iron in mammalian cells prefer the divalent iron (e.g., DMT1, ZIP8, ZIP14, ferroportin).

The mechanism underlying the function of this transport system in FAC-treated cells remains unexplainable at present. The transport system is functional in FAC-exposed cells without exogenous addition of Fe^{3+} to the extracellular medium. It is expected that the FAC-treated cells accumulate Fe^{3+} during treatment, but how this intracellular Fe^{3+} supports citrate uptake via the transport system remains unknown. Experiments with iron chelators clearly indicate that Fe^{3+} is available in the extracellular medium in FAC-treated cells without adding any exogenous source of Fe^{3+} to support Fe^{3+}-citrate uptake, but how Fe^{3+} exits the cells is not known. Experiments with the hepcidin mimetic rule out ferroportin in the process. Additional studies are needed to understand the molecular mechanism responsible for coupling intracellular Fe^{3+} to citrate uptake in FAC-treated cells via the Fe^{3+}-coupled citrate transport system.

Under physiological conditions, there is very little free iron in circulation; most of it is bound to transferrin. A recent study has estimated the plasma level of free iron to be less than 0.5 μM[22]. Even though the plasma levels of NTBI are normally very low, this pool increases significantly under conditions of iron overload. The plasma levels of NTBI increase substantially in various diseases related to iron overload, which include genetic disorders such as sickle cell disease and thalassemia[33,34] and hemochromatosis[35,36]. The increase is also seen in various conditions associated with defective erythropoiesis (myelodysplastic syndromes)[37] and repeated blood transfusion[38]. Even dietary iron overload is known to increase the circulating levels of NTBI[39]. The plasma levels of NTBI have been shown to increase several-fold (5 μM or higher) under iron-overload conditions[22]. Such concentrations of free Fe^{3+} are sufficient to activate the newly discovered citrate transport to a significant extent. While transferrin-bound iron is physiological and non-toxic, NTBI is toxic[40,41]. It is also becoming increasingly evident that NTBI is related to a wide spectrum of neurodegenerative diseases[42–44]. The newly discovered Fe^{3+}-citrate transport system is likely to play a critical role in the pathogenesis of NTBI toxicity.

There are numerous studies in the literature that describe uptake mechanisms for NTBI in mammalian cells[45–52]. In most of these studies, iron was presented to cells in the form of ferric citrate; apparently citrate was added to chelate Fe^{3+} and maintain the metal ion in a soluble form. In some studies, the uptake of not only iron but also citrate was monitored[48,50], but in none of the studies the effect of Na^+ was investigated. The overall conclusion from these studies is that mammalian cells possess one or more specific transport systems for iron uptake in a transferrin-independent manner, but there is no consensus as to the molecular identity of the transporters responsible for these uptake processes. But none of the studies in the literature proposes an NTBI transporter that accepts Fe^{3+} as the substrate; involvement of ferri-reductases that convert Fe^{3+} to Fe^{2+} before uptake via either ZIP8/ZIP14 or some other NTBI transporter is implicated in all of these studies. In contrast, the present study focused on citrate uptake and the involvement of Fe^{3+} in this uptake process. This approach has uncovered the presence of a novel transport system for citrate in mammalian cells that operates only in the presence of Fe^{3+} as well as Na^+ under physiological conditions.

Citrate is a key metabolite with multiple biological functions[53,54]. Most of citrate inside the cell is generated within the mitochondria by citrate synthase, which then feeds into the citric acid cycle for energy production. When cells have sufficient supply of ATP, citrate generated in mitochondria is used for anabolic functions. Citrate exits the mitochondria as most of the anabolic functions of citrate take place in the cytoplasm; the exit is mediated by the mitochondrial citrate transporter SLC25A1. Cytoplasmic citrate is a potent regulator of glycolysis as an allosteric inhibitor of the rate-limiting enzyme phosphofructokinase-1. Citrate is also the principal source of acetyl CoA in the cytoplasm, which is produced by the activity of ATP:citrate lyase. Acetyl CoA then serves as the carbon source for synthesis of fatty acids, cholesterol, dolichol, and isoprenoids. Normal plasma also contains significant levels of citrate, in the range of 150–200 μM[55]. Citrate present in the circulation can enter cells via NaCT and increase the cytoplasmic pool of citrate to impact on glycolysis and fatty acid/cholesterol synthesis[10]. The NaCT-knockout mice are resistant to diet-induced obesity and metabolic syndrome[6], underlining the importance of plasma citrate in hepatic fat metabolism and insulin sensitivity. Therefore, the newly discovered Na^+-coupled Fe^{3+}-citrate transport system, which facilitates the entry of citrate from the circulation into cells, particularly liver cells, has potential to impact the development and progression of a wide spectrum of diseases; this is specially so under conditions of iron overload where plasma levels of free iron increase to levels sufficient enough to activate the new citrate transport system to a significant extent to have biological impact.

On the other hand, the new citrate transport system might have therapeutic potential for children suffering from epilepsy and encephalopathy caused by loss-of-function mutations in NaCT. The clinical symptoms in these patients are obviously due to the inability of neuronal cells to take up citrate from the extracellular medium. The newly identified citrate transport system might not be very active under normal physiological conditions because

of the very low levels of free iron. It might be therapeutically beneficial to these patients if citrate could be provided to neurons bypassing the inactive NaCT. Ferric ammonium citrate is an FDA-approved iron supplement for children; when administered to children with NaCT mutations, this drug might increase the plasma levels of free iron sufficient enough to activate the Na^+-coupled Fe^{3+}-citrate transport system to facilitate citrate entry into affected neurons to compensate for the loss of function of NaCT. The rationale and validity of this idea remain however to be tested.

Methods

Materials. Ferric ammonium citrate (FAC), citrate, isocitrate, succinate, malate, lactate, pyruvate, deferiprone, and deferoxamine were purchased from Sigma-Aldrich (St. Louis, MO). The antibody for ferroportin was obtained from Abcam, Inc. (Cambridge, MA), which was raised against a peptide in human ferroportin. Radiolabeled citrate (1,5-[^{14}C]-citrate; specific radioactivity, 116.4 mCi/mmol) and radiolabeled Fe^{3+} ($^{59}FeCl_3$; specific radioactivity, >5 mCi/mg) were obtained from PerkinElmer (Waltham, MA). The sequences of the primers used in mRNA analysis and quantification for different citrate and iron/zinc transporters are listed in Supplemental Table 1.

Cell lines. HepG2 (a human hepatocellular carcinoma cell line), THLE-2 (a human normal hepatocyte cell line) and MCF7 (a human estrogen receptor-positive breast cancer cell line) were obtained from the American Tissue Culture Collection (ATCC, Manassas, MD). These cell lines were free of mycoplasma.

Primary hepatocytes. Primary hepatocytes were prepared from 6-week-old male mice using a procedure similar to what we described previously for the preparation of rat liver hepatocytes[9]. Nembutal (1 mg/kg body weight) was injected intraperitoneally for anesthetizing the animals. Heparin (5,000 IU/ml) was used as an anticoagulant, 0.1 ml of which was administered by injection into inferior vena cava. Portal vein was cannulated for liver perfusion. The first perfusion was with an EGTA-containing buffer (137 mM NaCl, 5.4 mM KCl, 0.5 mM NaH_2PO_4, 0.4 mM Na_2HPO_4, 4.2 mM $NaHCO_3$, 5 mM glucose, 0.5 mM EGTA, and 20 mM HEPES, pH 7.4), followed by the same buffer but containing 0.05% (wt/vol) collagenase, 0.005% (wt/vol) trypsin inhibitor, and 5 mM $CaCl_2$. The liver lobes were then resected and the cells dispersed in Krebs-Ringer buffer containing 3% bovine serum albumin and antibiotics. The dispersed cells were then filtered through cotton gauze and washed with the same buffer. Trypan blue was used to monitor cell viability, which was determined to be ~96%. Cells were then suspended in William's medium, supplemented with dexamethasone (1 nM), insulin (1 nM), 10% fetal bovine serum, and antibiotics. These final preparation of cells was used for uptake measurements. Cells were seeded in 24-well culture plates and allowed to attach to the culture wells for 4 h. Following this initial 4-h incubation, fresh culture medium was added and cultured for an additional 16 h at 37 °C in an incubator with 5% CO_2/95% air and then used for uptake measurements.

Uptake measurements. Cells were plated in 24-well culture plates in respective culture medium appropriate for each of the cell types. When FAC-exposed cells were used, FAC was used at the same concentration when the cells were cultured for uptake measurements. The medium was removed and replaced with fresh medium, again with or without FAC as appropriate, after 36 h. The next day (12 h following the medium change), the cells were used for uptake measurements. The medium was aspirated and the cells were washed twice with uptake medium, which was maintained at 37 °C, and then uptake was initiated by addition of radiolabeled citrate or radiolabeled Fe^{3+} in the uptake medium. Incubation of the cells with radiolabeled substrates was continued for 15 min, following which the medium was removed by aspiration, and the cells washed twice with ice-cold uptake medium. The cells were then solubilized with 1%SDS/0.2 N NaOH and used for measurement of radioactivity. The composition of the uptake medium in most cases was: 25 mM Hepes/Tris buffer (pH 7.5) containing 140 mM NaCl, 5.4 mM KCl, 0.8 mM $MgSO_4$, 1.8 mM $CaCl_2$, and 5 mM glucose[4,7,9]. When Na^+-free medium was required for uptake, NaCl in the medium was replaced iso-osmotically with *N*-methyl-D-glucamine (NMDG) chloride. The uptake measurements were made routinely in triplicates and the experiment was repeated at least three times. For each experiment, the concentration of protein was measured in one or two wells with cells cultured in the same 24-well plate under identical conditions as the cells used for uptake, which was used to normalize the uptake rate. In some experiments, the normalization was done with cell number instead of protein concentration.

Chronic exposure to excess iron in culture and impact of iron chelation on citrate uptake. FAC was used as the exogenous source of iron. Cells (HepG2, THLE-2, and MCF7) were cultured in medium appropriate for the respective cell lines in the absence or presence of FAC for two passages and then used for measurement of citrate uptake. The effects of iron chelation on citrate uptake in FAC-treated cells were studied using HepG2 cells. Iron chelation was done with deferiprone and deferoxamine under two different experimental conditions. First, FAC-treated HepG2 cells were used for citrate uptake in the presence of different concentrations of deferiprone (0.1–1 mM) or deferoxamine (0.25 mM). Second, FAC-treated HepG2 cells were washed twice with 1 mM deferoxamine and then citrate uptake was measured in the absence of deferoxamine.

Treatment of HepG2 cells with minihepcidin peptide and immunofluorescence analysis of ferroportin. Cells were seeded on chamber slides and cultured with regular culture medium. The next day, the culture medium was removed and replaced with fresh medium containing PR73 minihepcidin peptide at 1 μM and incubated for 24 h. Following this treatment, cells were washed and fixed with 1% paraformaldehyde for 30 min at 37 °C and then permeabilized with 0.1% Triton X-100 for 3 min. The cells were then incubated with 10% goat serum for 60 min to block non-specific interaction with the antibody. The cells were then stained with rabbit anti-SLC40A1 (ferroportin) antibody (ab78066 from Abcam; 5 μg/ml) overnight at 4 °C. Following this treatment, the cells were washed and then incubated with secondary antibody (goat anti-rabbit IgG) conjugated

with fluorescein isothiocyanate (Cat. No. 31583 from Thermo Fisher Scientific, Rockford, IL, USA; 15 μg/ml) for 60 min, and then washed and mounted with Prolog™ diamond antifade mounting medium. All images were captured using a Nikon ECLIPSE Ts2R inverted microscope (Tokyo, Japan).

Statistical analysis. All uptake experiments were repeated at least three times, each time measurements made in triplicate. Data (mean ± S. D.) are presented as percent of uptake in corresponding control cells. The actual value for control uptake is also given for each experiment. Multiple statistical comparisons were made by the one-way analysis of variance (ANOVA). Whenever appropriate, paired Student's t test was used to determine statistical significance between control and experimental datasets. $p < 0.05$ was considered statistically significant. The immunofluorescence experiment was repeated twice, both yielding similar results.

Use of experimental animals. All animal experiments reported here were carried out at the Texas Tech University Health Sciences Center and were approved by the Animal Care and Use Committee at that institution. All other experiments were performed in accordance with relevant guidelines and regulations.

Data availability. All of the data pertaining to this study are provided in the figures and supplementary material contained in this manuscript.

References

1. Bergeron, M. J., Clemencon, B., Hediger, M. A. & Markovich, D. SLC13 family of Na^+-coupled di- and tri-carboxylate/sulfate transporters. *Mol. Aspects Med.* **34**, 299–312 (2013).
2. Pajor, A. M. Sodium-coupled dicarboxylate and citrate transporters from the SLC13 family. *Pflugers Arch.* **466**, 119–130 (2014).
3. Rogina, B., Reenan, R. A., Nilsen, S. P. & Helfand, S. L. Extended lifespan conferred by cotransporter gene mutations in *Drosophila*. *Science* **290**, 2137–2140 (2000).
4. Inoue, K., Zhuang, L., Maddox, D. M., Smith, S. B. & Ganapathy, V. Structure, function, and expression pattern of a novel sodium-coupled citrate transporter (NaCT) cloned from mammalian brain. *J. Biol. Chem.* **277**, 39469–39476 (2002).
5. Rogers, R. P. & Rogina, B. The role of INDY in metabolism, health and longevity. *Front. Genet.* **6**, 204 (2015).
6. Birkenfeld, A. L. *et al*. Deletion of the mammalian INDY homolog mimics aspects of dietary restriction and protects against adiposity and insulin resistance in mice. *Cell Metab.* **14**, 184–195 (2011).
7. Inoue, K., Zhuang, L. & Ganapathy, V. Human Na^+-coupled citrate transporter: primary structure, genomic organization, and transport function. *Biochem. Biophys. Res. Commun.* **299**, 465–471 (2002).
8. Inoue, K. *et al*. Functional features and genomic organization of mouse NaCT, a sodium-coupled transporter for tricarboxylic acid cycle intermediates. *Biochem. J.* **378**, 949–957 (2004).
9. Gopal, E. *et al*. Expression and functional features of NaCT, a sodium-coupled citrate transporter, in human and rat livers and cell lines. *Am. J. Physiol. Gastrointest. Liver Physiol.* **292**, G402–G408 (2007).
10. Inoue, K., Zhuang, L., Maddox, D. M., Smith, S. B. & Ganapathy, V. Human sodium-coupled citrate transporter, the orthologue of *Drosophila* Indy, as a novel target for lithium action. *Biochem. J.* **374**, 21–26 (2003).
11. Thevenon, J. *et al*. *M*utations in SLC13A5 cause autosomal-recessive epileptic encephalopathy with seizure onset in the first days of life. *Am. J. Hum. Genet.* **95**, 113–120 (2014).
12. Hardies, K. *et al*. Recessive mutations in SLC13A5 result in a loss of citrate transport and cause neonatal epilepsy, developmental delay and teeth hypoplasia. *Brain* **138**, 3238–3250 (2015).
13. Schossig, A. *et al*. SLC13A5 is the second gene associated with Kohlschutter-Tonz syndrome. *J. Med. Genet.* **54**, 54062 (2017).
14. Weeke, L. C. *et al*. Punctate white matter lesions in full-term infants with neonatal seizures associated with SLC13A5 mutations. *Eur. J. Paediatr. Neurol.* **21**, 396–403 (2017).
15. Klotz, J., Porter, B. E., Colas, C., Schlessinger, A. & Pajor, A. M. Mutations in the Na^+/citrate cotransporter NaCT (SLC13A5) in pediatric patients with epilepsy and developmental delay. *Mol. Med.* **26**, 22 (2016).
16. Bainbridge, M. N. *et al*. Analyses of SLC13A5-epilepsy patients reveal perturbations of TCA cycle. *Mol. Genet. Metab.* **121**, 314–319 (2017).
17. Bhutia, Y. B., Kopel, J. J., Lawrence, J. J., Neugebauer, V. & Ganapathy, V. Plasma membrane Na^+-coupled citrate transporter (SLC13A5) and neonatal epileptic encephalopathy. *Molecules* **22**, E378 (2017).
18. Kopel, J. J. *et al*. Tooth hypoplasia for differential diagnosis of childhood epilepsy associated with SLC13A5 mutations. *Int. J. Neurol. Disord.* **1**, 33–37 (2017).
19. Yodoya, E. *et al*. Functional and molecular identification of sodium-coupled dicarboxylate transporters in rat primary cultured cerebrocortical astrocytes and neurons. *J. Neurochem.* **97**, 162–173 (2006).
20. Gopal, E. *et al*. Species-specific influence of lithium on the activity of SLC13A5 (NaCT): lithium-induced activation is specific for the transporter in primates. *J. Pharmacol. Exp. Ther.* **353**, 17–26 (2015).
21. Ito, S. *et al*. *In vivo* behavior of NTBI revealed by automated quantification system. *Int. J. Hematol.* **104**, 175–181 (2016).
22. Stefanova, D. *et al*. Endogenous hepcidin and its agonist mediate resistance to selected infections by clearing non-transferrin-bound iron. *Blood* **130**, 245–257 (2017).
23. Drakesmith, H., Nemeth, E. & Ganz, T. Ironing out Ferroportin. *Cell Metab.* **22**, 777–787 (2015).
24. Fung, E., Chua, K., Ganz, T., Nemeth, E. & Ruchala, P. Thiol-derivatized minihepcidins retain biological activity. *Bioorg. Med. Chem. Lett.* **25**, 763–766 (2015).
25. Liuzzi, J. P., Aydemir, F., Nam, H., Knutson, M. D. & Cousins, R. J. Zip14 (Slc39a14) mediates non-transferrin-bound iron uptake into cells. *Proc. Natl. Acad. Sci. USA* **103**, 13612–13617 (2006).
26. Pinilla-Tenas, J. J. *et al*. Zip14 is a complex broad-scope metal-ion transporter whose functional properties support roles in the cellular uptake of zinc and nontransferrin-bound iron. *Am. J. Physiol. Cell Physiol.* **301**, C862–C871 (2011).
27. Jenkitkasemwong, S. *et al*. SLC39A14 is required for the development of hepatocellular iron overload in murine models of hereditary hemochromatosis. *Cell Metab.* **22**, 138–150 (2015).
28. Jenkitkasemwong, S., Wang, C. Y., Mackenzie, B. & Knutson, M. D. Physiologic implications of metal-ion transport by ZIP14 and ZIP8. *Biometals.* **25**, 643–655 (2012).
29. Lensbouer, J. J. & Doyle, R. P. Secondary transport of metal-citrate complexes: the CitMHS family. *Crit. Rev. Biochem. Mol. Biol.* **45**, 453–462 (2010).
30. Korithoski, B., Krastel, K. & Cvitkovitch, D. G. Transport and metabolism of citrate by *Streptococcus mutans*. *J. Bacteriol.* **187**, 4451–4456 (2010).
31. Lensbouer, J. J., Patel, A., Sirianni, J. P. & Doyle, R. P. Functional characterization and metal ion specificity of the metal-citrate complex transporter from *Streptomyces coelicolor*. *J. Bacteriol.* **190**, 5616–5623 (2008).
32. Francis, A. J., Dodge, C. J. & Gillow, J. B. Biodegradation of metal citrate complexes and implications for toxic-metal mobility. *Nature* **356**, 140–142 (1992).

33. Porter, J. B. Pathophysiology of transfusional iron overload: contrasting patterns in thalassemia major and sickle cell disease. *Hemoglobin* **33**(Suppl. 1), S37–S45 (2009).
34. Marsella, M. & Borgna-Pignatti, C. Transfusional iron overload and iron chelation therapy in thalassemia major and sickle cell disease. *Hematol. Oncol. Clin. North Am.* **28**, 703–727 (2014).
35. Le Lan, C. *et al*. Redox active plasma iron in C282Y/C282Y hemochromatosis. *Blood* **105**, 4527–4531 (2005).
36. Ryan, E. *et al*. Correlates of hepcidin and NTBI according to HFE status in patients referred to a liver centre. *Acta Haematol.* **133**, 155–161 (2015).
37. Steensma, D. P. & Gattermann, N. When is iron overload deleterious, and when and how should iron chelation therapy be administered in myelodysplastic syndromes? *Best Pract. Res. Clin. Haematol.* **26**, 431–444 (2013).
38. Porter, J. B. & Garbowski, M. The pathophysiology of transfusional iron overload. *Hematol. Oncol. Clin. North Am.* **28**, 683–701 (2014).
39. McNamara, L. *et al*. Non-transferrin-bound iron and hepatic dysfunction in African dietary iron overload. *J. Gastroenterol. Hepatol.* **14**, 126–132 (1999).
40. Anderson, G. J. Non-transferrin-bound iron and cellular toxicity. *J. Gastroenterol. Hepatol.* **14**, 105–108 (1999).
41. Brissot, P., Ropert, M., Le Lan, C. & Loreal, O. Non-transferrin bound iron: a key role in iron overload and iron toxicity. *Biochim. Biophys. Acta* **1820**, 403–410 (2012).
42. Mills, E., Dong, X. P., Wang, F. & Xu, H. Mechanisms of brain iron transport: insight into neurodegeneration and CNS disorders. *Future Med. Chem.* **2**, 51–64 (2010).
43. Codazzi, F., Pelizzoni, I., Zacchetti, D. & Grohovaz, F. Iron entry in neurons and astrocytes: a link with synaptic activity. *Front. Mol. Neurosci.* **8**, 18 (2015).
44. Tripathi, A. K. *et al*. Transport of non-transferrin bound iron to the brain: implications for Alzheimer's disease. *J. Alzheimers Dis.* **58**, 1109–1119 (2017).
45. Basset, P., Quesneau, Y. & Zwiller, J. Iron-induced L1210 cell growth: evidence of a transferrin-independent iron transport. *Cancer Res.* **46**, 1644–1647 (1986).
46. Sturrock, A., Alexander, J., Lamb, J., Craven, C. M. & Kaplan, J. Characterization of a transferrin-independent uptake system for iron in HeLa cells. *J. Biol. Chem.* **265**, 3139–3145 (1990).
47. Kaplan, J., Jordan, I. & Sturrock, A. Regulation of the transferrin-independent iron transport system in cultured cells. *J. Biol. Chem.* **266**, 2997–3004 (1991).
48. Jordan, I. & Kaplan, J. The mammalian transferrin-independent iron transport may involve a surface ferrireductase activity. *Biochem. J.* **302**, 875–879 (1994).
49. Olakanmi, O., Stokes, J. B. & Britigan, B. E. Acquisition of iron bound to low molecular weight chelates by human monocyte-derived macrophages. *J. Immunol.* **153**, 2691–2703 (1994).
50. Kriegerbeckova, K., Dopper, L., Scheiber, B., Kovar, J. & Goldenberg, H. Non-transferrin iron uptake by HeLa cells cultured in serum-free media with different iron sources. *Eur. J. Clin. Chem. Clin. Biochem.* **33**, 791–797 (1995).
51. Richardson, D. R. Iron and gallium increase iron uptake from transferrin by human melanoma cells: further examination of the ferric ammonium citrate-activated iron uptake process. *Biochim. Biophys. Acta* **1536**, 43–54 (2001).
52. Ji, C. & Kosman, D. J. Molecular mechanisms of non-transferrin-bound and transferrin-bound iron uptake in primary hippocampal neurons. *J. Neurochem.* **133**, 668–683 (2015).
53. Ganapathy, V. & Fei, Y. J. Biological role and therapeutic potential of NaCT, a sodium-coupled transporter for citrate in mammals. *Proc. Ind. Natl. Sci. Acad.* **B71**, 83–96 (2005).
54. Mycielska, M. E., Milenkovic, V. M., Wetzel, C. H., Rummele, P. & Geissler, E. K. Extracellular citrate in health and disease. *Curr. Mol. Med.* **15**, 884–891 (2015).
55. Fraenkl, S. A. *et al*. Plasma citrate levels as a potential biomarker for glaucoma. *J. Ocul. Pharmacol. Ther.* **27**, 577–580 (2011).

Acknowledgements

This work was supported by the Welch Endowed Chair in Biochemistry, Grant No. BI-0028, at Texas Tech University Health Sciences Center.

Author Contributions

J.O., E.B., Y.D.B., S.M., and S.R. performed the experiments; E.N. and V.G. designed the experiments, interpreted the data, and prepared the manuscript.

Additional Information

Supplementary information accompanies this paper at https://doi.org/10.1038/s41598-018-20620-w.

Competing Interests: The authors declare that they have no competing interests.

Publisher's note: Springer Nature remains neutral with regard to jurisdictional claims in published maps and institutional affiliations.